PROCEEDINGS OF SCIENCE

Review of magnetospheric and space weather observations by the High-Energy Particle Detector (HEPD-01) on board the CSES-01 satellite

Francesco Palma[a,*] **and Matteo Martucci**[a] **for the Limadou/HEPD-01 Collaboration**

[a] *INFN-Sezione di Roma "Tor Vergata",*
Via della Ricerca Scientifica 1, I-00133 Roma, Italy

E-mail: francesco.palma@roma2.infn.it

Earth's magnetosphere is part of a dynamic, interconnected system which responds to solar, planetary, and interstellar conditions. It encloses two belts of magnetically trapped, energetic charged particles, which constitute a well-known hazard to spacecraft systems and crews, significantly constraining human activities in space. Despite notable improvements made in the latest decades, the modeling of the trapped environment is still incomplete, with largest uncertainties affecting the high-energy fluxes (> 50 MeV) in the inner regions and in the South Atlantic Anomaly (SAA). Additionally, space weather events increase the spatial and composition variability of the magnetospheric radiation belts, e.g. during geomagnetic storms. The Italian High-Energy Particle Detector (HEPD-01), on a low-Earth orbit since February 2018, is providing crucial new insight in the physical dynamics of the radiation belts, thus enabling an extensive testing and validation of current theoretical and empirical models of the near-Earth environment (e.g. AP9 and AE9). In this contribution, a review of magnetospheric and space weather observations by HEPD-01 is presented, including the study of some major geomagnetic storms, such as the G3-class ones of August 2018 and May 2021, the re-entrant lepton spectrum between 20 and 100 MeV and the proton fluxes inside the SAA in the 40-250 MeV energy range.

38th International Cosmic Ray Conference (ICRC2023)
26 July - 3 August, 2023
Nagoya, Japan

*Speaker

PoS(ICRC2023)1282

1. Introduction

Earth's geomagnetic cavity is a dynamic system generated by the effect of the solar wind and geomagnetic field and structured in several macro-regions, such as the ionosphere, magnetosphere, and Van Allen belts. The Van Allen belts are zones of energetic charged particles which are trapped in the Earth's magnetic field; the outer belt is mostly populated by electrons with hundreds of keV to MeV energies, while the inner belt mostly consists of a high concentration of energetic protons (from MeV up to a few GeV), electrons/positrons (up to ~ 10 MeV), and a minor component of ions. The outer Van Allen radiation belts are extremely variable in composition, especially when powerful solar energetic particle (SEP) events encounter the magnetic field lines, while the inner belt is more stable and less affected by solar activity. Additionally, the interaction between the galactic cosmic populations and the magnetosphere generates a set of particles called albedo (upward direction), which can be further identified either as re-entrant (if their trajectory is bent by the geomagnetic field, allowing them to remain trapped with a downward direction) or splash albedo (if they are able to escape the magnetosphere after the interaction with the atmosphere). Furthermore, the tilt of the geomagnetic field gives rise to a peculiar region, the South Atlantic Anomaly (SAA), centered over the eastern South America. The SAA is a region of lower geomagnetic field that causes the mirroring of the inner radiation belt particles at lower altitudes, increasing the local particle flux. It is thus the region where the inner radiation belt makes its closest approach to the Earth's surface (~ 200 km). Since the end of the commissioning phase in August 2018, the High-Energy Particle Detector (HEPD-01) on board the China Seismo-Electromagnetic Satellite (CSES-01) has been returning valuable information on the Sun-magnetosphere interaction and on the composition of the Van Allen belts.

2. The HEPD-01 detector on board the CSES-01 satellite

CSES-01 [1] is the first item of an extended constellation of low-Earth orbit (LEO) satellites, designed for the observation of perturbations in electromagnetic fields and waves, plasma parameters and charged particle fluxes, induced by both natural (earthquakes, solar events, cosmic rays, etc.) and anthropogenic sources in the near-Earth space. In order to achieve these goals, since February 2, 2018, CSES-01 has been flying on a Sun-synchronous polar orbit at a ~ 507 km altitude, a 97° inclination, and a ~ 5 day revisiting periodicity. Among the nine payloads on board CSES-01 is the High-Energy Particle Detector (HEPD-01), which was designed and built by the Limadou Collaboration, the Italian portion of the CSES mission. HEPD-01 is optimized for the detection of electrons and protons in the 3 – 100 MeV and ~ 30 - 300 MeV energy ranges, respectively, as well as the measurement of light nuclei. For this purpose, from top to bottom, HEPD-01 includes the following set of sub-detectors: a tracker made up of two double-sided silicon microstrip planes, a trigger system (T) including one plastic scintillator layer segmented into six paddles, a range calorimeter comprising a tower of 16 plastic scintillator planes (P1, P2, ..., P16) and a matrix of 3 × 3 lutetium–yttrium oxyorthosilicate (LYSO) inorganic scintillator crystals. Finally, the detector is equipped with an anti-coincidence (VETO) system composed of 5 plastic scintillator planes, out of which 4 are placed at the lateral sides of the apparatus and 1 at the bottom. For further details on the HEPD-01 detector and the CSES-01 mission, see [2–4] and references therein.

3. HEPD-01 observation of particles from outer radiation belts

Geomagnetic storms and sub-storms are among the most important signatures of the variability in the Sun-Earth environment. During the non-linear and extremely complicated processes that take place there, the Earth's magnetosphere is significantly affected by the perturbations originating from the Sun, such as coronal mass ejections (CMEs) or solar flares. As a consequence, changes can occur in the magnetosphere-ionosphere current systems and, in addition, a temporary rearrangement of the trapped particles in the radiation belts can take place, which can be subsequently observed by particle detectors at low-Earth orbits. Three strong geomagnetic storms have been observed

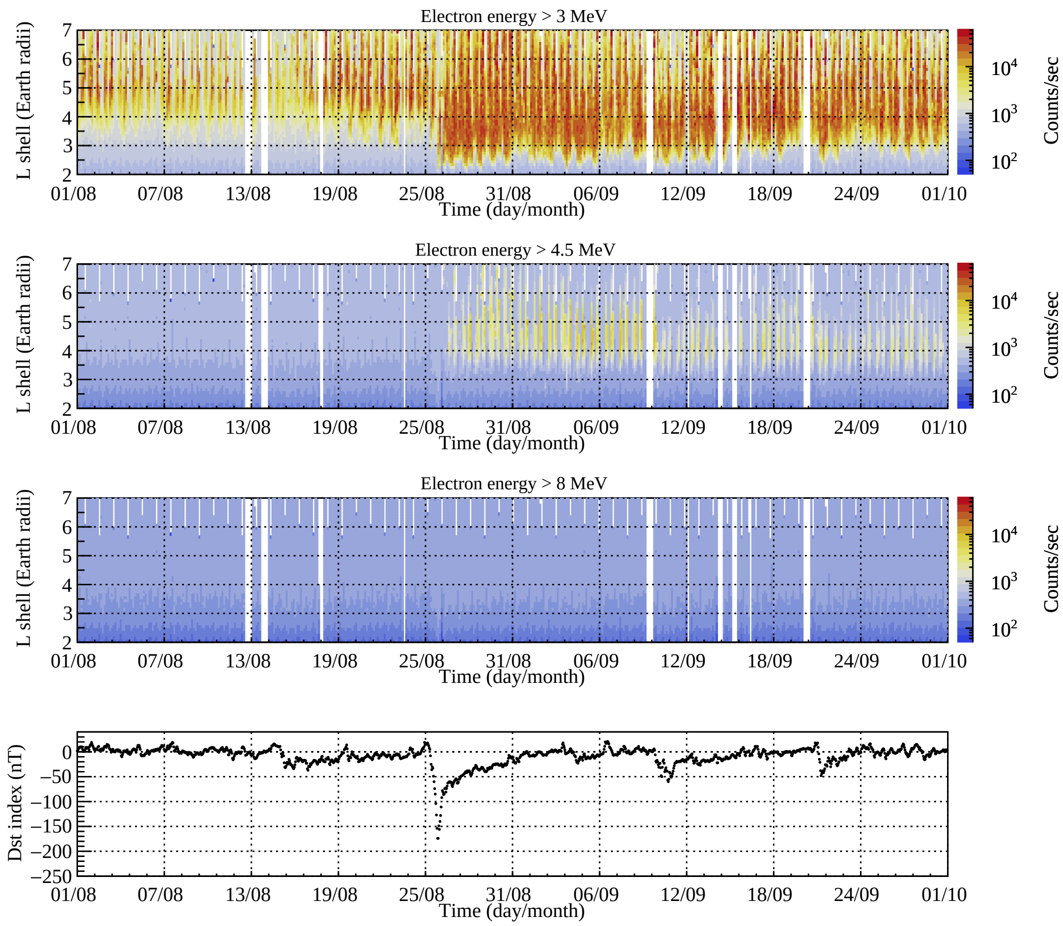

Figure 1: HEPD-01 particle rates corresponding to three different trigger configurations as a function of time during the G3-class geomagnetic storm of August 26, 2018 (marked by a strong decrease in the Dst index shown in the bottom panel): by increasing the number of planes used for the generation of the trigger, the energy threshold increases, showing that low-energy particles were the most affected by the storm, as expected.

by HEPD-01 so far during the CSES-01 mission: the two G3-class storms of August 26, 2018 and May 12, 2021 and the one of November 4, 2021. In all three cases, the geomagnetic storm was caused by the impact on the magnetosphere of a coronal mass ejection, which had been emitted from the Sun a few days earlier. Following the geomagnetic disturbance of August 26, 2018, which was characterized by marked magnetosphere compression and plasmasphere erosion, a clear enhancement of HEPD-01 particle rates during the storm's recovery phase was observed. In particular, this increase was visible at L-shells $\gtrsim 3$ for electron energies above 3 MeV (Figure 1, top panel), and, to a lesser extent, at L-shells $\gtrsim 4$ for electron energies above 4.5 MeV (Figure 1, middle panel), exactly in coincidence with a strong decrease of the Disturbance storm-time (Dst) index down to ~ -190 nT (Figure 1, bottom panel). This enhancement in HEPD-01 trigger rates suggested a phenomenon of magnetospheric electron acceleration, which lasted for several days and was associated with a prolonged and intense substorm activity (see [5] for a detailed discussion). Conversely, during the May 12, 2021 storm, HEPD-01 registered a sudden and persistent loss of relativistic electrons from the entire outer radiation belt (Figure 2, bottom panel), whose very rapid, non-recovering dropout can only be the result of non-adiabatic processes permanently removing particles from the system. One of these processes can likely be the magnetopause shadowing

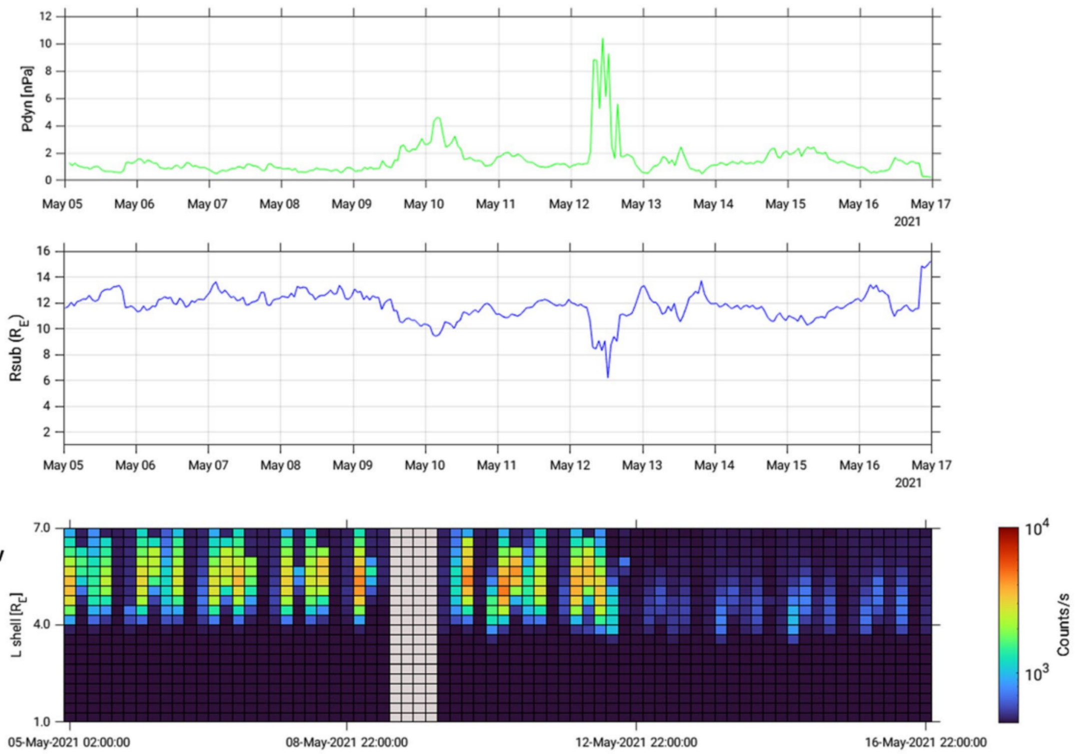

Figure 2: Top two panels: time profile of the solar wind dynamic pressure and position of the magnetopause standoff distance over the period of 5–16 May 2021, respectively; bottom panel: rates of > 4.5 MeV particles detected by HEPD-01 over the same period. Gray shaded areas refer to time intervals for which HEPD-01 data are not available.

in combination with outward radial transport [6], as suggested by the perfect match between the deep magnetopause incursion on L-shells no higher than ~ 6.2 R_E around 12:50 UTC of May 12 (Figure 2, middle panel) and the abrupt ten-fold increment in solar wind dynamic pressure over the same time interval (Figure 2, top panel). Finally, the latest geomagnetic storm detected by HEPD-01 took place on November 4, 2021, a week after the October 28 X1.0 class solar flare, which produced the first ground-level enhancement of the 25$^{\text{th}}$ solar cycle [7]. The HEPD-01 detector observed

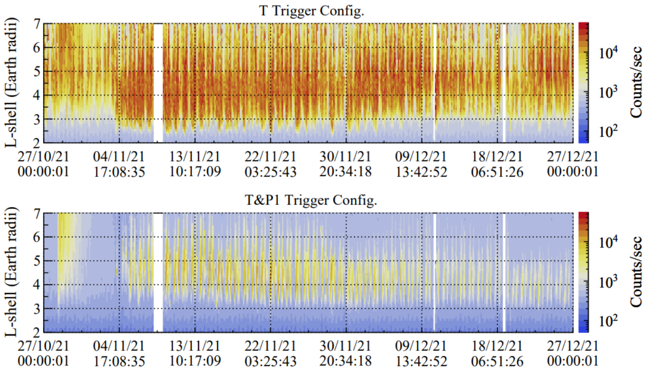

Figure 3: HEPD-01 particle rates corresponding to two different trigger configurations as a function of time during the geomagnetic storm of November 4, 2021.

both the SEP event and the subsequent geomagnetic storm, as it is evident in the bottom panel of Figure 3 exhibiting two well-separated increases in the HEPD-01 trigger rates. The left yellow spot around October 28 marks the increase in the particle rate due to the injection of solar protons as a consequence of the flare, then the particle rate comes back to normal levels and, finally, a new enhancement is evident as a consequence of the magnetospheric electron redistribution during the geomagnetic storm hitting the Earth.

4. HEPD-01 observation of re-entrant albedo leptons

As already mentioned, the magnetospheric radiation also includes populations of re-entrant albedo particles originated by the collisions of cosmic rays with the outermost layers of the atmosphere. Figure 4 shows the re-entrant all-electron differential flux measured by HEPD-01 between

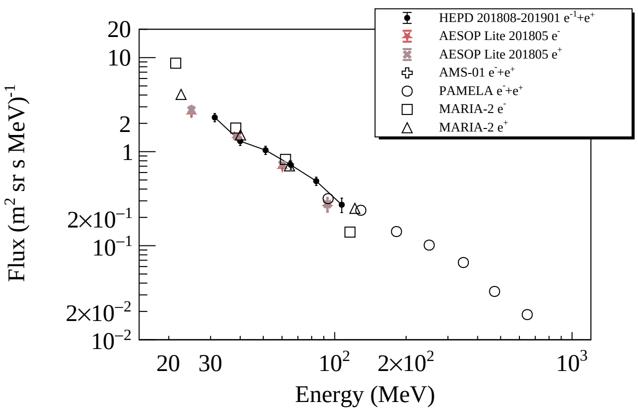

Figure 4: Re-entrant all-electron differential spectrum measured by HEPD-01 between 2018 and 2022 (black filled circles) and compared with other experiments.

20 and 100 MeV outside the SAA (B > 23000 nT) and at 1.1 < L-shell < 1.2. The resulting spectrum appears in very good agreement with results from previous experiments. Moreover, eight six-month re-entrant lepton spectra between 20 and 100 MeV have been obtained from data gathered in the

period 2018-2022 and for five different L-shell intervals (Figure 5). As expected, these spectra result quite stable in time, while they increase when moving to higher L-shell values.

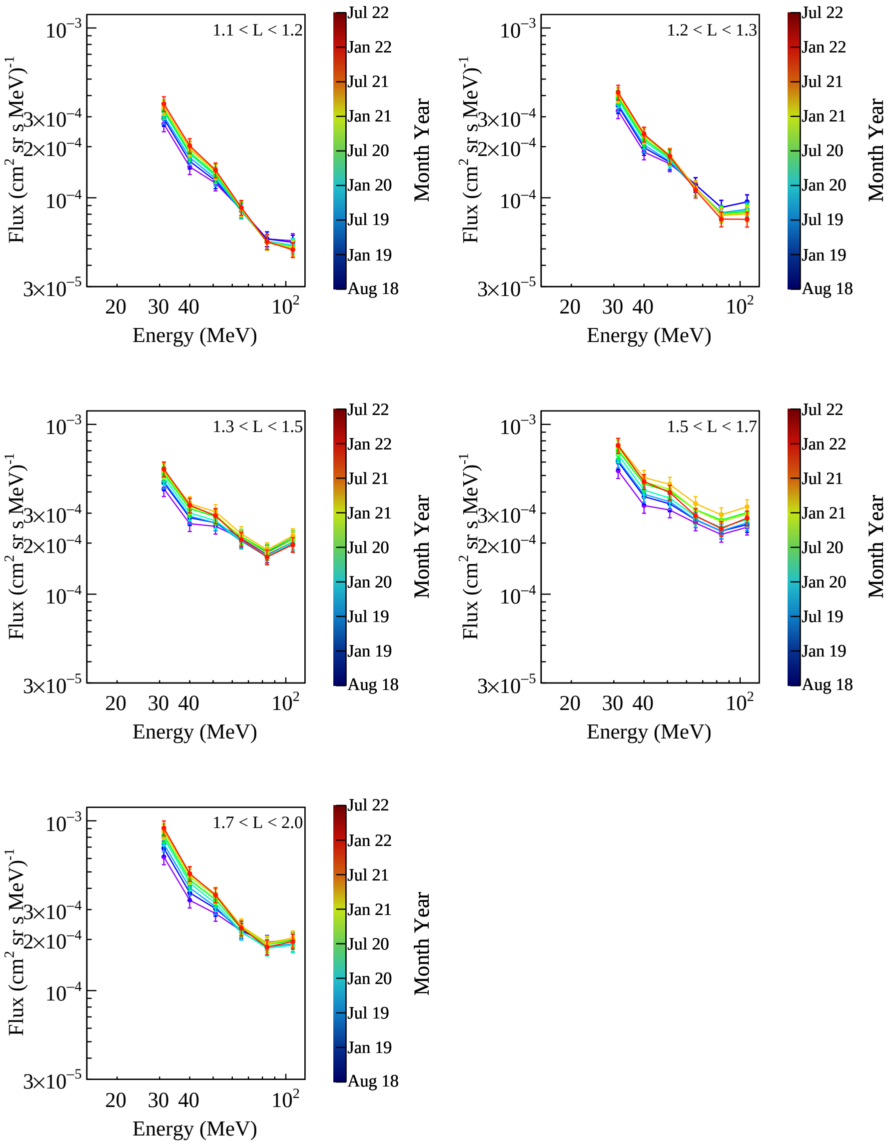

Figure 5: Each panel contains eight re-entrant all-electron spectra between 20 and 100 MeV, each related to a 6-month time period - see color-coded palette. Moreover, each panel refers to a different L-shell interval, labelled in the top-right corner of each panel.

5. HEPD-01 observation of protons inside the South Atlantic Anomaly

Finally, the HEPD-01 detector provided the first results on protons inside the SAA at low-Earth orbit during the minimum activity phase between the 24$^{\text{th}}$ and the 25$^{\text{th}}$ solar cycles in the energy range 40 MeV-250 MeV [8]. The data are in generally good agreement with the AP9 model at

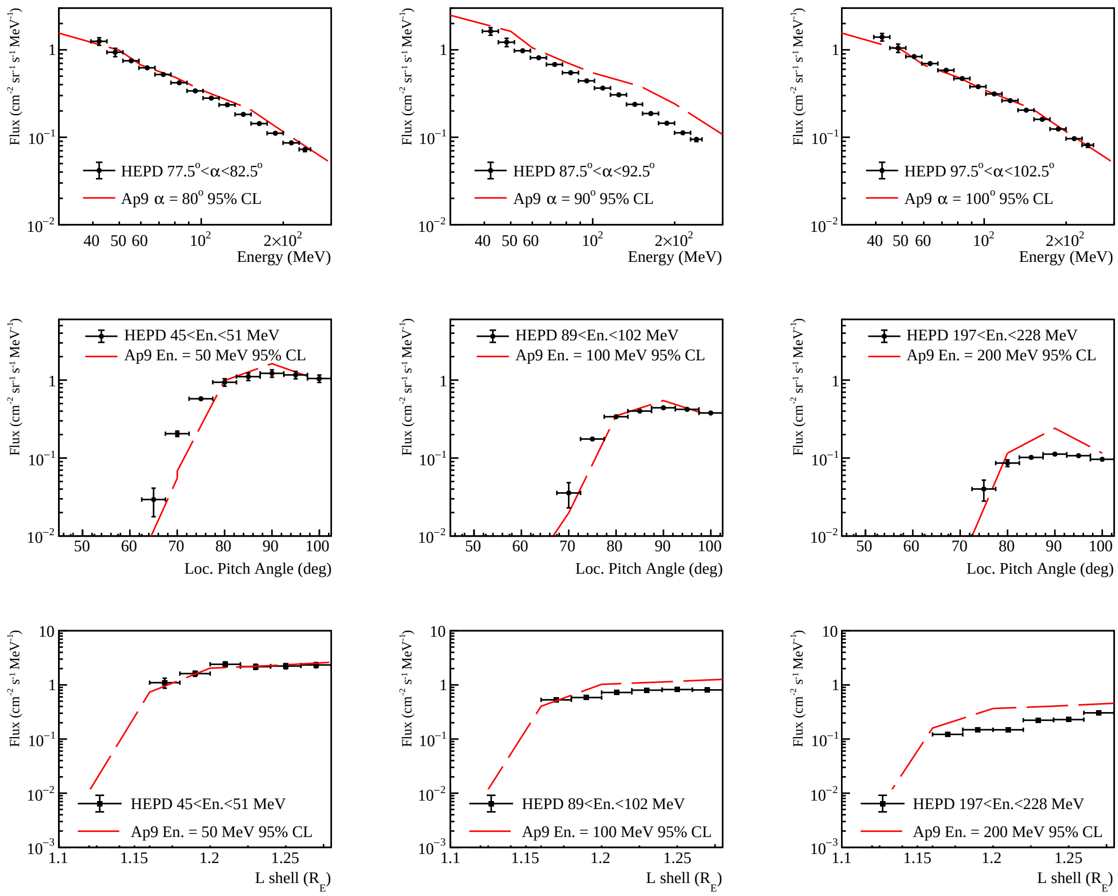

Figure 6: SAA proton fluxes as a function of energy (top panels), local pitch angle (middle panels) and L-shell (bottom panels) obtained by HEPD-01 (black squares) between August 2018 and December 2020, and compared with predictions from the AP9 model at 95% confidence level (red dashed lines).

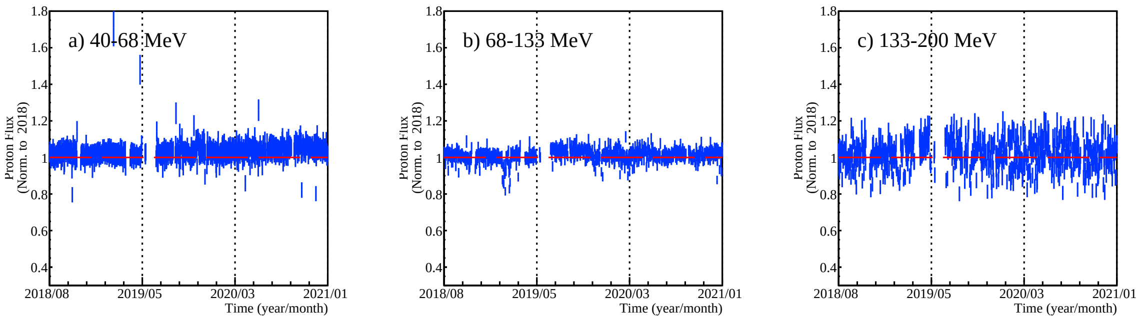

Figure 7: Time profiles (1-day time binning) of omnidirectional protons inside the SAA measured by HEPD-01 from August 2018 to December 2020, normalized to the month of August 2018. The three panels refer to three different energy ranges: low (40 MeV– 68 MeV, left panel), medium (68 MeV–133 MeV, middle panel) and high (133 MeV–200 MeV, right panel). The gap in proton data between May 2019 and June 2019 refers to a period of instrument malfunctioning.

95% confidence level, as a function of energy (Figure 6, top panels), local pitch angle (Figure 6, middle panels), and L-shell (Figure 6, bottom panels). Moreover, the time-intensity profiles of the proton fluxes in three different energy ranges appear to be constant over time (Figure 7), as foreseen for the phase of the solar cycle in which the data have been collected (between mid 2018 and late 2020, with a number of sunspots close to zero).

6. Conclusions

Since August 2018, the HEPD-01 instrument has been contributing to the study of the complex near-Earth radiation environment. In particular, HEPD-01 data have proven very useful to monitor the electron redistribution in the Earth's magnetosphere as a consequence of solar perturbations, such as during the three reported geomagnetic storms. Moving to lower L-shells, a back-tracing analysis is ongoing to separate the different populations of re-entrant albedo electrons and protons, while results on SAA-trapped protons have already provided an excellent cross-calibration for radiation models in such a critical region. These results are even more valuable considering the forthcoming launch of the HEPD-02 detector on board the CSES-02 satellite.

References

[1] X. Shen and et al., *The state-of-the-art of the china seismo-electromagnetic satellite mission*, *Science China Technological Sciences* **61** (2018) .

[2] P. Picozza and et al., *Scientific goals and in-orbit performance of the high-energy particle detector on board the cses*, *The Astrophysical Journal Supplement Series* **243** (2019) 16.

[3] G. Ambrosi and et al., *Beam test calibrations of the HEPD detector on board the China Seismo-Electromagnetic Satellite*, *Nuclear Instruments and Methods in Physics Research A* **974** (2020) 164170.

[4] G. Ambrosi and et al., *The electronics of the High-Energy Particle Detector on board the CSES-01 satellite*, *Nuclear Instruments and Methods in Physics Research A* **1013** (2021) 165639.

[5] F. Palma and et al., *The august 2018 geomagnetic storm observed by the high-energy particle detector on board the cses-01 satellite*, *Applied Sciences* **11** (2021) .

[6] M. Piersanti and et al., *On the Magnetosphere-Ionosphere Coupling During the May 2021 Geomagnetic Storm*, *Space Weather* **20** (2022) e2021SW003016.

[7] M. Martucci and et al., *The First Ground-Level Enhancement of Solar Cycle 25 as Seen by the High-Energy Particle Detector (HEPD-01) on Board the CSES-01 Satellite*, *Space Weather* **21** (2023) e2022SW003191.

[8] M. Martucci and et al., *New results on protons inside the south atlantic anomaly, at energies between 40 and 250 mev in the period 2018–2020, from the cses-01 satellite mission*, *Phys. Rev. D* **105** (2022) 062001.

PoS(ICRC2023)1282

Full Authors List: Limadou/HEPD-01 Collaboration

S. Bartocci[a], R. Battiston[b,c], W. J. Burger[c], D. Campana[d], G. Castellini[e], P. Cipollone[a], L. Conti[f,a], A. Contin[g,h], C. De Donato[a], C. De Santis[a], F. M. Follega[b,c], G. Gebbia[b,c], R. Iuppa[b,c], M. Lolli[h], M. Martucci[a], G. Masciantonio[a], M. Mergè[i,a], M. Mese[l,d], C. Neubüser[c], F. Nozzoli[c], A. Oliva[h], G. Osteria[d], L. Pacini[m], F. Palma[a], F. Palmonari[g,h], B. Panico[l,d], F. Perfetto[d], P. Picozza[n,a], M. Pozzato[h], E. Ricci[b,c], M. Ricci[o], S. B. Ricciarini[e], Z. Sahnoun[g,h], V. Scotti[l,d], A. Sotgiu[a], R. Sparvoli[n,a], V. Vitale[a], S. Zoffoli[i] and P. Zuccon[b,c]

[a]INFN-Sezione di Roma "Tor Vergata", Via della Ricerca Scientifica 1, I-00133 Roma, Italy
[b]University of Trento, Via Sommarive 14, I-38123 Povo (Trento), Italy
[c]INFN-TIFPA, Via Sommarive 14, I-38123 Povo (Trento), Italy
[d]INFN-Sezione di Napoli, Via Cintia, I-80126 Napoli, Italy
[e]IFAC-CNR, Via Madonna del Piano 10, I-50019 Sesto Fiorentino (Firenze), Italy
[f]Uninettuno University, Corso V. Emanuele II 39, I-00186 Roma, Italy
[g]University of Bologna, Viale Berti Pichat 6/2, Bologna, Italy
[h]INFN-Sezione di Bologna, Viale Berti Pichat 6/2, Bologna, Italy
[i]Italian Space Agency, Via del Politecnico, I-00133 Roma, Italy
[l]University of Napoli "Federico II", Via Cintia, I-80126 Napoli, Italy
[m]INFN-Sezione di Firenze, Via Sansone 1, I-50019 Sesto Fiorentino (Firenze), Italy
[n]University of Roma "Tor Vergata", Via della Ricerca Scientifica 1, I-00133 Roma, Italy
[o]INFN-LNF, Via E. Fermi 54, I-00044 Frascati (Roma), Italy